ENERGY QUIPSYS

Energy Equipment and Systems

Thermoeconomic analysis of a hybrid PVT solar system integrated with double effect absorption chiller for cooling/hydrogen production

Authors

Amirmohammad Behzadi[a]
Ehsan Gholamian[a]
Ehsan Houshfar[a*]
Mehdi Ashjaee[a]
Ali Habibollahzade[a]

[a]School of Mechanical Engineering, College of Engineering, University of Tehran, P.O. Box 11155-4563, Tehran, Iran

ABSTRACT

A novel solar-based combined system which is consisting of a concentrated PV, a double effect LiBr-H_2O absorption chiller, and a Proton Exchange Membrane (PEM) is proposed for hydrogen production. A portion of the received energy is recovered to run a double effect absorption chiller and the rest is turned into electricity, being consumed in the PEM electrolyzer for hydrogen production. The thermodynamic and thermoeconomic analyses are performed to understand the system performance. A parametric study which is implementing Engineering Equation Solver (EES) is carried out to assess the influence of main decision parameters on the overall exergy efficiency and total product unit cost. The 2nd law analysis shows that PVT with exergy destruction rate of 76.9% of total destruction rate is the major source of irreversibility. Furthermore, in the cooling system, Cooling Set (CS) has the highest exergy destruction rate due to the dissipative components. Exergoeconomic results demonstrate that in cooling set with the lowest value of exergoeconomic factor, the cost of exergy destruction and loss has the major effect on the overall cost rate. Furthermore, results of the parametric study indicate that by decreasing PV cell's temperature from 100 °C to 160 °C, the total product unit cost is decreased by about 1.94 $/GJ.

1. Introduction

The extra use of fossil fuels has led to various issues toward climate change, global warming, and greenhouse gases emission. The renewable energies such as solar, wind, biomass, and geothermal which need more attentions and

proper policies from the governments, are the alternative scenarios. Recently, in the Paris climate agreement, all of the countries agreed to reduce their carbon emission and implement renewable energies as their major source of energy [1]. The world bank and International Energy Agency (IEA) predicted that, the world needs two folds of the current installed capacity for proving the next 40 years electrical power [2]. Therefore, more focus is needed on developing

---
* Corresponding author: Ehsan Houshfar
School of Mechanical Engineering, College of Engineering, University of Tehran, P.O. Box 11155-4563, Tehran, Iran
Email: houshfar@ut.ac.ir

all kind of renewable energy sources to reduce the fossil fuel consumption. In this research work, a novel solar-based cogeneration energy system is proposed that consists of a photovoltaic/thermal, a double effect absorption chiller, and a PEM electrolyzer.

1.1. Photovoltaic/Thermal system

Solar energy is the most available and the cleanest source among all kind of renewable energy resources. Solar energy technologies are divided into passive and active technologies. Photovoltaic cells are one of the examples of active technologies, which convert the originated heat and light of the sun into electricity. The reduction of cells temperature leads to better Photo Voltaic (PV) performance and therefore a higher efficiency [3]. Photo Voltaic/Thermal (PVT) technology is a common method to achieve this target by recovering waste heat for other consumptions [4]. Gaur and Tiwari [5] investigated the effect of cell temperature on the overall efficiency by using water as the coolant. They showed that water increases the thermal efficiency and daily average electrical power by about 7.5% and 4.8%, respectively. Notton *et al.* [6] evaluated the effect of physical variables of the PV cell material, the module and the environment condition on the performance of PV cell.

1.2. Double effect absorption chiller

An absorption cooling system, which has a proper consistency with the solar energy plants, can be used to recover the low grade waste heat [7]. Energy and exergy analysis of a single effect and a double effect absorption chiller was compared by Gomri [8]. He studied the variation of cooling load and exergy destruction rate of each component with major parameter, concluding that the COP of the single effect absorption chiller is half of the COP of the double effect absorption chiller. The exergoeconomic evaluation was proposed by Garousi Farshi *et al.* [9] to improve the effective cost of the system due to the high prices of the evaporator and absorber of double effect absorption chiller.

1.3. Hydrogen production

Due to the global warming and high amount of greenhouse gas emission, it is necessary to introduce a novel, clean, and environmentally friendly energy source as a substitute for fossil fuels. Recently, a large number of researchers using different methods have investigated on hydrogen production. Khanmohammadi *et al.* [10] analyzed a renewable based energy system for hydrogen production using the exergoeconomic technique. They carried out a parametric study to evaluate the effect of important parameters on hydrogen production rate and objective functions of the system. Penkuhn *et al.* [11] investigated exergetic and exergoeconomic analysis of a small-scale PEM electrolyzer, which produces hydrogen for mobile and stationary off-grid applications. They compared the costs of irreversibility and the investment costs to show the source of high cost of electricity.

1.4. Cogeneration system

Eisavi *et al.* [12] analyzed a novel which has been combined cooling, heating, and power system based on solar energy from the first and second law of thermodynamics point of view. They concluded that using double-effect absorption chiller instead of single effect leads to 48.5% increase in the cooling capacity. The comparison of combined cooling, heating and power system (CCHP) integrated with PVT panels with internal combustion engine was proposed by Yousefi *et al.* [13]. The results of the thermodynamic and thermoeconomic analysis showed that using CCHP system with solar energy, results in a better system performance. Akrami *et al.* [14] investigated exergy and exergoeconomic assessments of single-effect absorption cooling system with hydrogen production unit which has been driven by PVT. They found that the major source of irreversibility is the PVT with 80% of the total exergy destruction rate. Furthermore, it was stated that, the High-Pressure Generator (HPG) has the highest exergy destruction rate in absorption cooling systems. In addition, the results of the exergoeconomic analysis revealed that PVT is the most important unit with a capital investment cost of 0.0895 $/h. In a recent study, Moradi Nafchi *et al.* [15] investigated the performance assessment of an integrated system which is consisting of a PEM, a concentrating solar power, and a thermal energy storage. They proposed that hydrogen production efficiency is by 23.1%, while electricity efficiency is by 45%. Furthermore, they showed that exergy destruction is about 5% due to the conversion of electricity to hydrogen production. Hydrogen production of

PEM driven by the solar collector was simulated by Omar and Altinişik [16]. They implemented the parametric study to evaluate the effect of pressure and temperature on the system performance. The study concluded that the effect of pressure on hydrogen and oxygen production system could be neglected. A power/hydrogen generation system which consists of an ORC and a PEM electrolyzer was analyzed by Nami and Akrami [17] from the energy and exergy point of view. The results of the parametric study showed that an increase in superheating temperature of the turbine lowers the rate of hydrogen production. Additionally, they showed that steam, power and hydrogen production cost are equal to 20.56 $/ton, 4.81 cents/kWh, and 3.97 $/kg of hydrogen, respectively.

To the best of our knowledge, there is no comprehensive research that has investigated the hydrogen and cooling production from a PVT system which has been equipped with the double effect absorption cooling system from the exergy and exergoeconomic viewpoints. Hence, in the current study, energy, exergy, and exergoeconomic analysis of a cogeneration system consisting of PVT, a PEM electrolyzer, and a double effect absorption cooling system is presented in detail. The main objectives and novelties of this research can be summarized as:

- Increasing the thermal efficiency of PVT by utilizing the waste heat recovery.
- Implementing a PEM electrolyzer to use excess electricity to produce hydrogen using PVT power output.
- Using a double effect absorption cooling system for cooling production by utilizing the waste heat of PVT.
- Applying energy, exergy, and exergoeconomic assessment of the proposed cycle to evaluate the system performance.
- Identifying the most important components from exergy destruction and capital investment cost perspectives.

Nomenclature

A	The cross section area (m^2)
c	Concentrated ratio
c	Cost per unit exergy ($/GJ)
$\dot{C}$	Cost rate ($/hr)
C_P	Specific heat capacity at constant pressure (kJ/kgK)
E	Exergy (kJ)
$\dot{E}$	Exergy rate (kW)
$E_{act,i}$	Activation energy (kJ/kmol)
f	Exergoeconomic factor
F	Faraday constant
$\varDelta G$	Gibbs free energy (kJ)
G	Direct solar radiation (kW/m^2)
h	Specific enthalpy (kJ/kg)
i_r	Interest rate
J	Current density (A/m^2)
$J_{0,i}$	Exchange current density (A/m^2)
J_i^{ref}	Pre-exponential factor (A/m^2)
l	Thickness (m)
$\dot{m}$	Mass flow rate (kg/s)
P	Pressure (kPa)
$\dot{Q}$	Heating load (kW)
Q_{Conv}	Heat convected to the atmosphere (kW)
Q_{pv}	Net incident concentrated solar radiation on the PV module (kW)
Q_{rad}	Heat radiated to the atmosphere (kW)
Q_{Th}	Heat absorbed by the PV cells (kW)
R	Ideal gas constant (kJ/kgK)
s	Specific entropy (kJ/kg.K)
T_{gl}	Cover glass temperature (°C)
T_{ins}	Insulation temperature (°C)
T_{PV}	Cell's temperature (°C)
T_{ref}	Cell's reference temperature (°C)
T_{Sky}	Sky temperature (°C)
T_{Sun}	The sun temperature (°C)
u_{Wind}	Wind velocity (m/s)
V	Voltage (v)
V_0	Reversible potential (v)
$\dot{W}$	Power (kW)
X_i	Mole fraction of the ith component
Z	Investment cost of components ($)
$\dot{Z}$	Investment cost rate of component ($/hr)

Subscript and abbreviations

0	Dead state
a	Atmosphere
1,2,3,…,	State points
Abs	Absorber
act,a	activation overpotential of the anode
act,c	activation overpotential of the cathode
an	anode
Ch	Chemical
CI	Capital investment
COND	Condenser
COP	Coefficient of performance
CS	Cooling set
CRF	Capital recovery factor
E.V	Expansion valve
f	fuel
HPG	High Pressure Generator
HTHEX	High temperature heat exchanger
i	inlet
L	Loss

l   liquid
LPG   Low Pressure Generator
LTHEX Low temperature heat exchanger
o   outlet
ohm   Ohmic overpotential of the electrolyte
OM   Operation and maintenance
PEM   Proton exchange membrane
PVT   Photovoltaic/Thermal
P   Product
Ph   Physical
Pm   Pump
tot   total

Greek Symbols

η Efficiency
η_{inv} Inverter's efficiency
η_{is} Isentropic efficiency
η_{OPT} Optimal efficincy
η_{PV} Module's efficiency
η_{Tref} Module's efficiency at reference time
$\mathcal{E}_i$ Exergy efficiency of the ith component
τ Annual plant operation hours (hr)
σ Stefan-Boltzman constant (kW/m^{2}K)
λ Content of water
$\lambda(x)$ Content of water at distance of x
λ_{an} Content of water at anode membrane
λ_{ca} Content of water at cathode membrane

2. Cycle description and assumptions

A schematic diagram of the proposed cogeneration cycle is shown in Fig. 1 The system consists of three parts: the PVT system, the PEM electrolyzer, and the double effect LiBr-H$_2$O absorption chiller. As shown in Fig. 1, solar radiation is concentrated via reflector on the non-tracking PVT. A portion of the received energy is utilized to produce a cooling effect by the high-pressure generator of the absorption chiller (Q_{PVT}).Another portion is dissipated to the environment via convection and radiation. The rest is transformed into electricity power (P_{PV}) and utilized in the PEM to produce hydrogen.The following assumptions are considered for the proposed co-generation cycle:

- The proposed system is working under the steady-state conditions.
- Changes are neglected in potential and kinetic energies.
- There is no pressure drop in the pipes and heat exchangers.
- The condensation and absorption temperature is equal to 35 °C and the generator temperature is equal to 130 °C.
- The outlet water from the evaporator and condenser is saturated vapor and liquid, respectively.
- The heat exchangers effectiveness is by 70% in the cooling system.
- The surface area, concentration ratio, and cell temperature of the PVT are 1 m^2, 10 and 140 °C, respectively.

Fig.1. Schematic of the proposed cogeneration cycle consisting of PVT, absorption chiller, and PEM electrolyzer.

3. Mathematical modeling

Engineering Equation Solver (EES) package is implemented to perform the energy, exergy, and exergoeconomic analysis of the proposed cogeneration cycle. The detailed procedure and the governing equations are described in the following sections.

3.1. Energy and exergy analysis

Considering each component as a control volume, conservation of mass, energy, and exergy is applied to perform the mathematical modeling and thermodynamic analysis. Conservation of mass and energy equation for the Table 1. Also further information about the modeling of the PVT can be found in the literature [19].

The theoretical energy required for water electrolysis is defined as:

$$\Delta H = \Delta G + T \Delta S \tag{4}$$

where ΔG and $T\Delta S$ are Gibbs free energy and thermal energy, respectively. Outlet hydrogen mass flow rate from the electrolyzer is calculated by [20]:

$$\dot{m}_{H_2,out} = \dot{m}_{H_2O,reacted} = \frac{J}{2F} \tag{5}$$

where J and F are the current density and Faraday constant, respectively.

Taking V as the voltage of the PEM electrolyzer, required electricity for hydrogen production can be calculated from:

$$E_{electrical} = JV \tag{6}$$

$$V = V_0 + \eta_{act,a} + \eta_{act,c} + \eta_{ohm} \tag{7}$$

where V_0, $\eta_{act,a}$, $\eta_{act,c}$, and η_{ohm} are reversible potential, activation overpotential of anode, activation overpotential of cathode, and the ohmic overpotential of the electrolyte,

steady state condition which have been neglected potential and kinetics energies are [18]:

$$\sum \dot{m}_{in} = \sum \dot{m}_{out} \tag{1}$$

$$\sum \dot{m}_{in} X_{in} = \sum \dot{m}_{out} X_{out} \tag{2}$$

$$\dot{Q} - \dot{W} = \sum \dot{m}_{out} h_{out} - \sum \dot{m}_{in} h_{in} \tag{3}$$

where $\dot{W}$ and $\dot{Q}$ denote the rate of work and heat transfer, respectively. The total required energy for the PVT can be calculated by the equations tabulated in

respectively. The subscripts a and c denote anode and cathode, respectively. Reversible potential can be written as [20]:

$$V_0 = 1.229 - 8.5 \times 10^{-4}(T_{PEM} - 298) \tag{8}$$

In addition, local ionic conductivity of the membrane are expressed as [20]:

$$\sigma(\lambda(x)) = (0.5139\lambda(x) - 0.326) \times exp(12\ 68(1/303 - 1/T)) \tag{9}$$

where x denotes the membrane depth measured from the cathode interface. $\lambda(x)$ (content of water at distance x) is measured by:

$$\lambda(x) = (\lambda_{an} - \lambda_{ca})x/l + \lambda_{ca} \tag{10}$$

where l denotes thickness of the membrane, and λ_{an} and λ_{ca} are contents of water at anode and cathode membrane interface, respectively.

Furthermore, using ohmic's law, total ohmic resistance and the ohmic overpotential can be determined with Eqs. (11) and (12) [20].

$$R_{PEM} = \int_0^L \frac{dx}{\sigma(\lambda(x))} \tag{11}$$

$$\eta_{ohm} = JR_{PEM} \tag{12}$$

Table 1. Energy analysis of the PVT [19].

Component	Energy principles	Input parameters
	$Q_{Sun} = GC\eta_{opt} A$	$\eta_{PV} = \eta_{Tref}[1 - \beta_{ref}(T_C - T_{ref})]$
	$P_{PV} = Q_{PV}\eta_{PV}\eta_{inv}$	$\eta_{opt} = 0.85,\ \eta_{inv} = 0.9,\ \eta_{Tref} = 0.12$
	$Q_{Th} = Q_{PVT} + Q_{rad} + Q_{conv}$	$\beta = 0.004\,C^{-1},\ T_{ref} = T_0$
PVT	$Q_{Th} = Q_{Sun}(1 - \eta_{PV})$	$T_{Sky} = 0.0552\,T_a^{1.5}$
	$Q_{conv} = hA(T_{gl} - T_a) + hA(T_{ins} - T_a)$	$h = 2.8 + 3\,u_{Wind}$
	$Q_{rad} = \sigma\varepsilon A[(T_{gl}^4 - T_a^4) + (T_{ins}^4 - T_{Sky}^4)]$	$u_{Wind} = 2\,m/s,\ T_a = T_0$

Defining $J_{0,i}$ as the exchange current density, the activity of the electrodes is determined by activation overpotential as follows [21]:

$$\eta_{act,i} = \frac{RT}{F} sinh^{-1}\left(\frac{J}{2J_{0,i}}\right) =$$
$$\frac{RT}{F} ln\left(\frac{J}{2J_{0,i}} + \sqrt{\left(\frac{J}{2J_{0,i}}\right)^2 + 1}\right) \quad (13)$$

$$J_{0,i} = J_i^{ref} exp\left(-\frac{E_{act,i}}{RT}\right) \quad (14)$$

where J_i^{ref} and $E_{act,i}$ denote the pre-exponential factor and the activation energy for the anode and cathode, respectively. The constant parameters in the modeling of PEM electrolyzer can be found in the literature [20, 21]. Beyond the conservation, exergy analysis focuses on the irreversibility and the quality of energy transfer [22]. The exergy balance equation is initially applied to each component to achieve the second law analysis [23]:

$$\dot{E}_Q - \dot{E}_W = \sum \dot{m}_{out} e_{out} - \sum \dot{m}_{in} e_{in} + \dot{E}_D \quad (15)$$

where $\dot{E}_Q$, $\dot{E}_W$, and $\dot{E}_D$ denote the rate of exergy that related to the heat transfer, work, and destruction for each component as a control volume. Neglecting the potential and kinetic exergies, the specific exergy is divided into physical and chemical, as follow [24]:

$$e = e^{ph} + e^{ch} \quad (16)$$

$$e_i^{ph} = (h_i - h_0) - T_0(s_i - s_0) \quad (17)$$

$$e_i^{ch} = \sum_{i=1}^{n} x_i e_{0,i}^{ch} + RT_0 \sum_{i=1}^{n} x_i \ln(x_i) \quad (18)$$

One of the most important objectives of the exergy analysis is to clarify the component with the highest value of exergy destruction as the main source of irreversibility., For a better exergoeconomic analysis, it is required to define the exergy of fuel and product for each component as tabulated in Table 2. Furthermore, the exergetic efficiency for each component is calculated by [25]:

$$\varepsilon_i = \frac{\dot{E}_{P,i}}{\dot{E}_{F,i}} \quad (19)$$

3.2. Exergoeconomic assessment

Exergoeconomic assessment combines the exergy analysis and economic principles, as described in this section. The cost balance for each component is written as follows [26]:

$$\sum \dot{C}_{e,k} + \dot{C}_{w,k} = \sum \dot{C}_{i,k} + \dot{C}_{q,k} + \dot{Z}_k \quad (20)$$

$$\dot{Z}_k = \dot{Z}_k^{CI} + \dot{Z}_k^{OM} \quad (21)$$

$$\dot{C}_i = c_i \cdot \dot{E}_i \quad (22)$$

$$\dot{C}_e = c_e \cdot \dot{E}_e \quad (23)$$

$$\dot{C}_q = c_q \cdot \dot{E}_q \quad (24)$$

$$\dot{C}_w = c_w \cdot \dot{W} \quad (25)$$

where $\dot{C}$ and c denote the cost rate in \$/h and the unit exergy cost rate in \$/GJ, respectively. In addition, subscripts i, e, w, and q in Eq. (20) denote the inlet, outlet, power, and heat transfer, respectively. The total cost rate ($\dot{Z}$) is the sum of capital investment costs and operating and maintenance costs which are calculated in Eq. (26) and Eq. (28), respectively:

Table 2. Defination of fuel, product, and loss exergy flowrates of the proposed cogeneration cycle components.

Component	Fuel	Product	Loss
PVT	$\dot{E}_{18}$	$\dot{E}_{QPVT} + \dot{E}_{19}$	–
HPG	$\dot{E}_{QPVT}$	$\dot{E}_{11} + \dot{E}_8 - \dot{E}_7$	–
LPG	$\dot{E}_{11} - \dot{E}_{12}$	$\dot{E}_{14} + \dot{E}_{15} - \dot{E}_{10}$	–
CS	$\dot{E}_{12} + \dot{E}_{14} + \dot{E}_9 + \dot{E}_{16} - \dot{E}_4 - \dot{E}_{10}$	$\dot{E}_{23} - \dot{E}_{22}$	$\dot{E}_{21} - \dot{E}_{20} + \dot{E}_{25} - \dot{E}_{24}$
Pump	$\dot{W}_{Pm}$	$\dot{E}_5 - \dot{E}_4$	–
HTHEX	$\dot{E}_8 - \dot{E}_9$	$\dot{E}_7 - \dot{E}_6$	–
LTHEX	$\dot{E}_{15} - \dot{E}_{16}$	$\dot{E}_6 - \dot{E}_5$	–
PEM electrolyzer	$\dot{E}_{19} + \dot{E}_{27}$	$\dot{E}_{31} + \dot{E}_{32}$	–

$$\dot{Z}_k^{CI} = \left(\frac{CRF}{\tau}\right) Z_k \qquad (26)$$

$$CRF = \frac{i_r (1+i_r)^n}{(1+i_r)^n - 1} \qquad (27)$$

$$\dot{Z}_k^{OM} = \gamma_k Z_k \qquad (28)$$

In Eq. (18), τ is the annual plant operation hours and CRF denotes the capital recovery factor. As shown in Eq. (19), the capital recovery factor will be calculated knowing the interest rate (i_r) and the number of year of plant operation (n). In present study, the annual plane operation hours and interest rate are

equal to 7920 h and 0.15, respectively. Furthermore, in Eq. (20) γ_k denotes the fixed operation and maintenance costs. The value of Z_k for each component is listed in Table 3. Marshal and Swift equation cost index is implemented to convert the value of $\dot{Z}_k$ substituted in Eq. (20) from reference year into the present year (2018) as follow [27]:

$$Cost\ at\ present\ year = original\ cost \times$$

$$\frac{Cost\ index\ for\ the\ present\ year}{Cost\ index\ for\ the\ year\ of\ original\ cost} \qquad (29)$$

Finally, cost balance and auxiliary equations for each component are listed in Table 4 to determine the cost rate per unit of exergy.

Table 3. Expression of purchase cost (Z_k) [28].

Component	Z_k ($)
PVT	$Z_{PVT} = c_0 A_{PVT}$ $c_0 = 1000\ \$/m^2$
HPG	$Z_{HPG} = c_1 (\frac{A_{HPG}}{A_0})^{0.6}$ $A_0 = 100\ m^2,\ c_1 = 17500\$$
LPG	$Z_{LPG} = c_1 (\frac{A_{LPG}}{A_0})^{0.6}$
Pump	$Z_{Pm} = c_2 \dot{W}_{Pm}^{0.65}$ $c_2 = 1000\ \$/kW^{0.65}$
HTHEX	$Z_{HTHEX} = c_3 (\frac{A_{HTHEX}}{A_0})^{0.6}$ $c_3 = 12000\ \$$
LTHEX	$Z_{LTHEX} = c_3 (\frac{A_{LTHEX}}{A_0})^{0.6}$
Evaporator	$Z_{Evap} = c_4 (\frac{A_{Evap}}{A_0})^{0.6}$ $c_4 = 16000\ \$$
Absorber	$Z_{ABS} = c_4 (\frac{A_{ABS}}{A_0})^{0.6}$
Condenser	$Z_{Cond1} = c_5 (\frac{A_{Cond}}{A_0})^{0.6}$ $c_5 = 8000$
PEM electrolyzer	$Z_{PEM} = c_6 \dot{W}_{PEM}$ $c_7 = 1000\ \$/(kW)$

Table 4. Cost balance and auxilary equations for components of proposed cycle [28, 29]

Component	Cost balance	Auxiliary equation
PVT	$\dot{C}_{18}+\dot{Z}_{PV}=\dot{C}_{19}+\dot{C}_{QPV}$	$c_{18}=0$
HPG	$\dot{C}_7+\dot{C}_{QPV}+\dot{Z}_{HPG}=\dot{C}_8+\dot{C}_{11}$	$\dfrac{\dot{C}_{11}}{\dot{m}_{11}(e_{11}-e_7)}=\dfrac{\dot{C}_7(e_8-e_{11})}{\dot{m}_7(e_{11}-e_7)(e_8-e_7)}+\dfrac{\dot{C}_8}{\dot{m}_8(e_8-e_7)}$
LPG	$\dot{C}_{11}+\dot{C}_{10}+\dot{Z}_{LPG}=\dot{C}_{14}+\dot{C}_{15}+\dot{C}_{12}$	$\dfrac{\dot{C}_{14}}{\dot{m}_{14}(e_{14}-e_{10})}=\dfrac{\dot{C}_{10}(e_{15}-e_{14})}{\dot{m}_{10}(e_{14}-e_{10})(e_{15}-e_{10})}+\dfrac{\dot{C}_{15}}{\dot{m}_{15}(e_{15}-e_{10})}$
CS	$\dot{C}_{14}+\dot{C}_{13}+\dot{Z}_{COND}=\dot{C}_1+\Delta\dot{C}_{COND}$ $\dot{C}_3+\dot{C}_{17}+\dot{Z}_{ABS}=\dot{C}_4+\Delta\dot{C}_{ABS}$ $\dot{C}_{12}+\dot{C}_{14}+\dot{C}_9+\dot{C}_{16}$ $+\dot{Z}_{ABS}+\dot{Z}_{COND}+\dot{Z}_{EVAP}+3\dot{Z}_{E.V}=$ $\Delta\dot{C}_{COND}+\Delta\dot{C}_{ABS}+\dot{C}_{23}-\dot{C}_{22}+\dot{C}_4+\dot{C}_{10}$	$\dfrac{\dot{C}_{13}+\dot{C}_{14}}{\dot{E}_{13}+\dot{E}_{14}}=\dfrac{\dot{C}_1}{\dot{E}_1}$ $\dfrac{\dot{C}_3+\dot{C}_{17}}{\dot{E}_3+\dot{E}_{17}}=\dfrac{\dot{C}_4}{\dot{E}_4}$ $c_1=c_2,\ c_2=c_3,\ c_9=c_{10}$ $c_{12}=c_{13},\ c_{16}=c_{17},\ c_{22}=c_{23}$
Pump	$\dot{C}_4+\dot{C}_{26}+\dot{Z}_{Pm}=\dot{C}_5$	$c_{19}=c_{26}$
HTHEX	$\dot{C}_6+\dot{C}_8+\dot{Z}_{HTHEX}=\dot{C}_7+\dot{C}_9$	$c_8=c_9$
LTHEX	$\dot{C}_5+\dot{C}_{15}+\dot{Z}_{LTHEX}=\dot{C}_6+\dot{C}_{16}$	$c_{15}=c_{16}$
PEM electrolyzer	$\dot{C}_{27}+\dot{C}_{19}+\dot{Z}_{PEM}=\dot{C}_{31}+\dot{C}_{32}$	$c_1=0$

For determining exergoeconomic parameters, the unit cost of fuel ($c_{F,k}$) and the unit cost of the product ($c_{P,k}$) are used [30]:

$$c_{F.k}=\frac{\dot{C}_{F.k}}{\dot{E}_{F.k}} \qquad (30)$$

$$c_{P.k}=\frac{\dot{C}_{P.k}}{\dot{E}_{P.k}} \qquad (31)$$

$$\dot{C}_{D.k}=c_{F.k}\dot{E}_{D.k} \qquad (32)$$

$$\dot{C}_{L.k}=c_{F.k}\dot{E}_{L.k} \qquad (33)$$

$$f_k=\frac{\dot{Z}_k}{\dot{Z}_k+\dot{C}_{D.k}+\dot{C}_{L.k}} \qquad (34)$$

Equation (34) determines the exergoeconomic factor to compare the importance of capital and operating and maintenance costs against costs of irreversibility.

3.3. Performance examination

Thermodynamic and thermoeconomic assessments are conducted for evaluating the Coefficient Of Performance (COP), overall exergy efficiency, and total product cost unit in $/GJ for the cogeneration system.

$$COP=\frac{\dot{Q}_e}{\dot{Q}_{PVT}} \qquad (35)$$

$$\eta_{II}=\frac{\dot{E}_{31}+\left(\dot{E}_{22}-\dot{E}_{23}\right)}{\dot{E}_{18}} \qquad (36)$$

$$c_{P,total}=\frac{\dot{C}_{31}+\dot{C}_{22}-\dot{C}_{23}}{\dot{E}_{31}+\dot{E}_{22}-\dot{E}_{23}} \qquad (37)$$

where $\dot{E}_{18}$ is the rate of exergy that is originated from the sun and is calculated as follows [31]:

$$\dot{E}_{18}=\left[1-\left(\frac{4T_0}{3T_S}\right)(1-0.28\ln f)\right]\dot{Q}_{Sun} \qquad (38)$$

T_S is the sun temperature (5778 K [32]) and f is the dilution factor which is equal to 1.3×10^{-5}.

4. Results and discussion

Parametric study is carried out to evaluate the effect of major parameters on system performance, economic and emission indicants

in detail. In addition, exergy destruction rate and the exergoeconomic factor is evaluated and discussed for every component.

4.1.Model Verification

To validate the results of this study, the PEM electrolyzer and PVT models are validated against available data in the literature.In Table 5 the variation of recovered heat from the PVT with concentration ratio is compared to the work of Kosmadakis et al. [19]. According to the table, there is a decent agreement between the results. Furthermore, for the PEM electrolyzer section, the comparison of the present model with experimental results from literature [33] is shown in Fig.2.The figure

reveals a good agreement between the results of the present model and literature.

In the Parametric study, initially, the effect of HPG and LPG temperatures is investigated on the Coefficient Of Performance (COP) of the double effect absorption chiller. In addition, the effect of PV module area and direct solar radiation is studied as major decision variables on the overall exergy efficiency and total unit product cost. In Fig. 3, the variation of COP with T_{LPG} for cooling cycle is shown at different T_{HPG}. Fig. 3 reveals that as the T_{LPG} increases from 75 °C to 95 °C, the COP is increased about 36%, which should be justified because of the decrease in the generator heating load. Unlike T_{LPG}, when the T_{HPG} increases, the generator thermal load rises so the COP drops.

Table 5. The variation of recovered heat from the PVT (kW) at different conccentration ratios in the present model vs. Kosmadakis et al. results [19]

Concentration ratio	Present model	Kosmadakis et al. [19]	Difference (%)
2	0.513	0.495	3.63
5	2.867	2.76	3.87
10	6.791	6.92	−1.8
15	10.72	10.85	−1.19
20	14.64	14.92	−1.87
40	30.33	31.13	−2.56
60	45.99	46.5	−1.1
100	77.32	79.18	−2.3
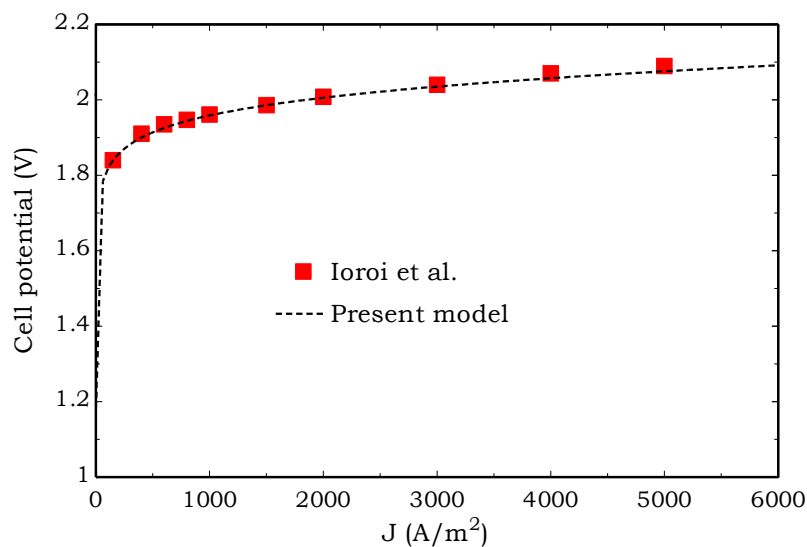
Fig. 2. Comparison of the present model with the exprimental data Parametric study
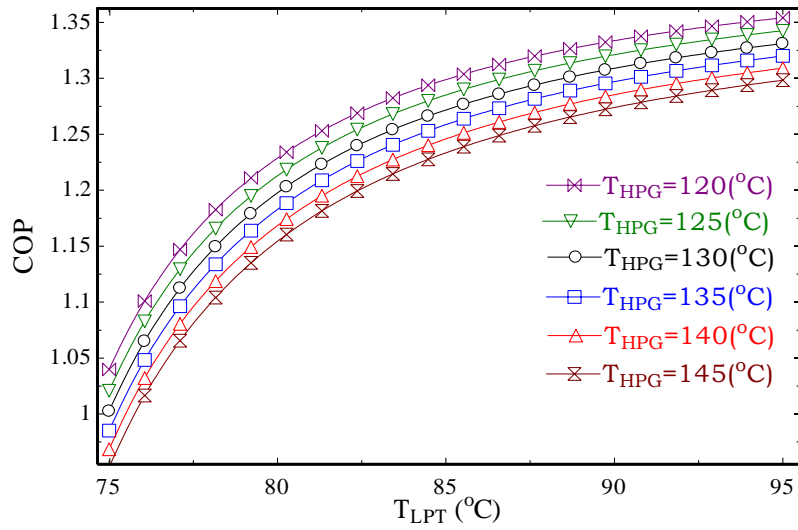
Fig.3. Variation of COP with T_{LPG} at different T_{HPG}

Figure 4 indicates the variation of overall exergy efficiency and total product unit cost with the PV module area. It can be inferred from Fig. 4 that the overall exergy efficiency increases with an increase in the PV module area up to a certain area and then it starts to decrease. Furthermore, by increasing the PV module area, the total product unit cost is decreased considerably from 70 \$/GJ to 30 \$/GJ.

Figure 5 shows the effect of direct solar radiation on the overall exergy efficiency and the total product unit cost. As the direct solar radiation increases from 0.2 kW/m^2 to 0.46 kW/m^2, the overall exergy efficiency is increased unnoteworthy and then it can be considered fixed. Furthermore, by increasing solar radiation from 0.2 kW/m^2 to 1.2 kW/m^2, the total product unit cost has got a noticeable decrease about 140.79 \$/GJ. From Fig. 4 and Fig. 5, it can be concluded that the PV module area and direct solar radiation have major effects on the thermoeconomic performance of the cogeneration system.
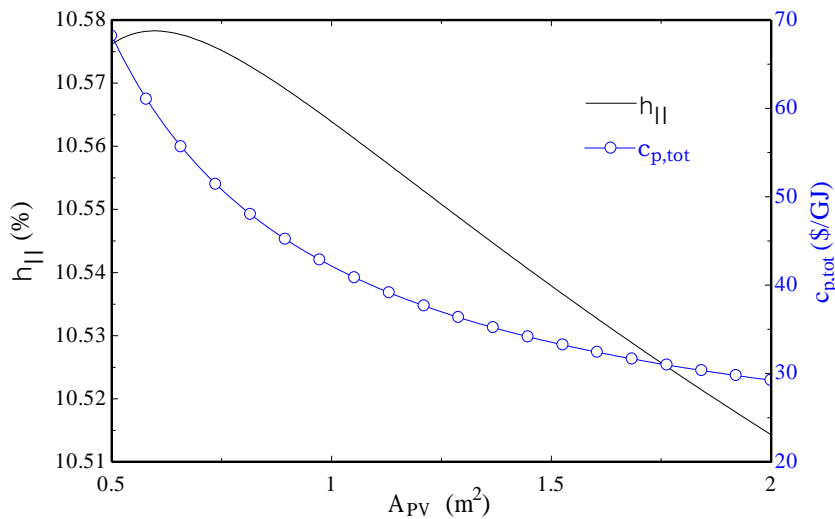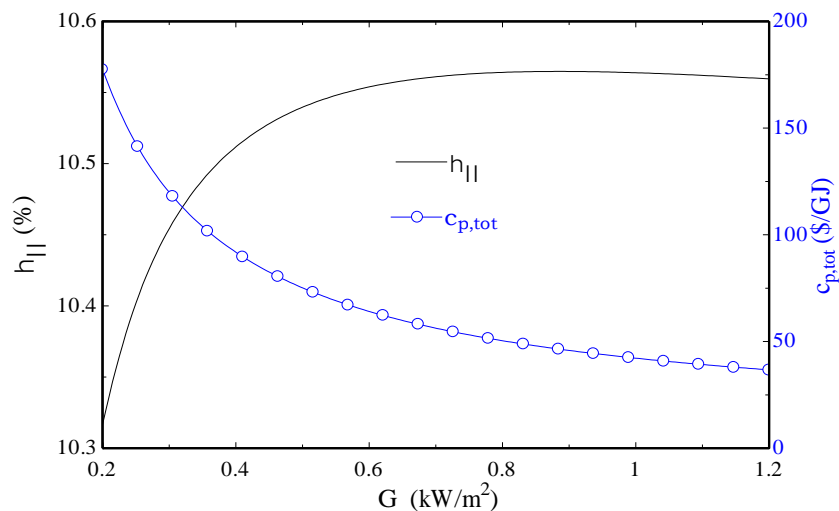

Fig.4. Variation of the overall exergy efficiency and the total product unit cost with the PV module area

Fig.5. Effect of the direct solar radiation on the overall exergy efficiency and the total product unit cost

Figure 6 shows that recovering waste heat of the PV has a positive effect on the performance of the PV and overall system from the thermodynamic and thermoeconomic point of view. Figure 6 exhibits that a higher PV cell's temperature leads to a lower overall exergy efficiency and higher total product unit cost, accordingly. When the PV cell's temperature increases from 100 °C to 160 °C, the PV thermal efficiency increases, therefore, the overall exergy efficiency drops by about 13%, while the total product unit cost increases about 1.94 $/GJ.

4.2. Exergy and exergoeconomic analysis

The results of exergy and exergoeconomic analysis are presented in this section.Table 6 represents the important thermodynamic and thermoeconomic variables at each state, i.e. the exergy rate in kW and exergy cost in $/GJ.

The exergy destruction and exergetic efficiency of each component is demonstrated in Fig. 7. Figure 7 (a) indicates that the LPG has the lowest exergy destruction rate with the rate of 0.0882 kW. In the cooling system, the HPG and dissipative components (cooling set) are considered as the significant components with approximately 72.75% of the total exergy destruction rate. It can clearly be concluded from Fig. 7 (a), that the PVT is the essential component from the irreversibility viewpoint with 76.9% of the total exergy destruction rate. Referring to the Fig. 7 (b), LPG has the highest 2nd law efficiency which is due to the lower temperature differences in comparison to the other heat exchangers. In addition, the PVT part with less than 34% has the lowest exergetic efficiency, which confirms the high irreversibility and exergy destruction within the section.
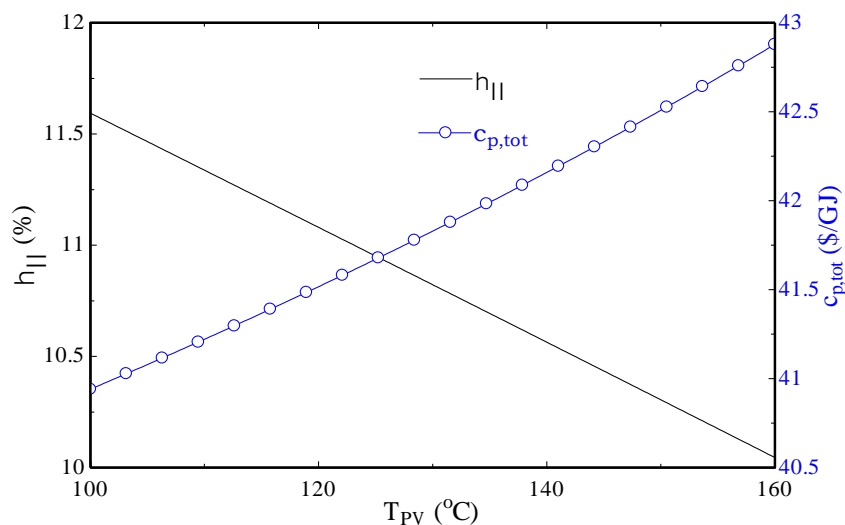
Fig.6. Variation of the overall exergy efficiency and the total product unit cost with the PV cell's temperature

Table 6. Exergy and unit cost at different point.

| Stream	$\dot{E}$ (kW)	c ($/GJ)	$\dot{C}$($/h)
1	0.002338	25.71	0.0002164
2	−0.02646	25.71	−0.002449
3	−0.7351	25.71	−0.06804
4	1.68	32.83	0.1985
5	1.68	40.03	0.2421
6	1.929	44.93	0.312
7	2.675	49.21	0.4739
8	3.731	35.36	0.4749
9	2.797	35.36	0.3561
10	2.797	35.36	0.3561
11	0.8461	9.99	0.03043
12	0.04226	9.99	0.00152
13	0.01445	9.99	0.0005198
14	0.1671	27.07	0.01628
15	3.345	31.08	0.3743
16	2.989	31.08	0.3344
17	2.989	31.08	0.3344
18	7.915	0	0
19	0.4957	10	0.01785
20	0.006619	0	0
21	0.0838	97.1	0.02929
22	0.5448	48.66	0.09544
23	1.058	48.66	0.1853
24	0.01523	0	0
25	0.1928	120	0.08328
26	0.01	10	0.02556
31	0.1829	51.44	0.03387
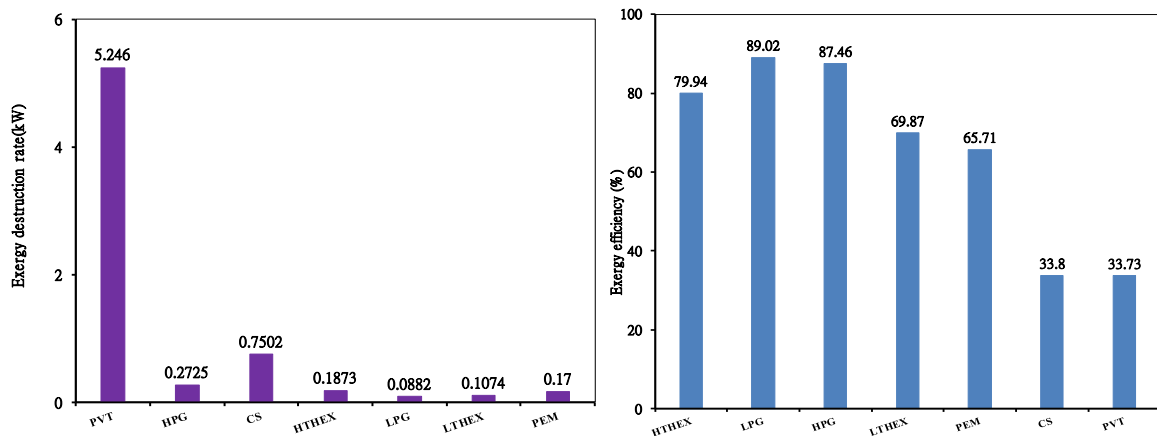
Fig.7. (a) Exergy destruction rate (b) exergetic efficiency by each component of the cogeneration system

Table 7. Exergy and exergoeconomic parameters of the cogeneration system.

Component	$\dot{E}_F$ (kW)	$\dot{E}_P$ (kW)	$\dot{E}_D$ (kW)	$\dot{E}_L$ (kW)	ε (%)	$\dot{C}_D$ ($/h)	$\dot{C}_L$ ($/h)	$\dot{Z}$ ($/h)	f (%)
PVT	7.915	2.669	5.246	0	33.73	0	0	0.04064	100
HPG	2.174	1.901	0.2725	0	87.46	0.002858	0	0.00862	75.11
LPG	0.8038	0.7156	0.0882	0	89.02	0.003173	0	0.00558	63.76
CS	1.518	0.5132	0.7502	0.2548	33.8	0.07593	0.02579	0.04882	32.43
Pump	0.01	0.01	0	0	100	0	0	0.01802	100
HTHEX	0.9337	0.7464	0.1873	0	79.94	0.02385	0	0.04305	64.35
LTHEX	0.3565	0.2491	0.1074	0	69.87	0.01202	0	0.03001	71.4
PEM	0.4957	0.3257	0.17	0	65.71	0.00612	0	0.01917	75.8
Overall system	7.915	0.836	6.8214	0.2576	10.56	0.12395	0.02579	0.21391	60.31

Exergoeconomic parameters are represented in Table 7, such as the cost of exergy destruction, exergy loss, capital cost, O&M (operating and maintenance) cost, and exergoeconomic factor for each component. The exergoeconomic factor, which plays an important role in the exergoeconomic evaluation, denotes the significance of capital and operating and maintenance cost against the cost rate of irreversibility. A low f denotes that the main part of the cost rate for the component is due to the cost of exergy destruction. Therefore, a better system performance can be achieved by reducing the irreversibility by allocating more money on the capital and investment costs. On the contrary, a higher f exhibits the major effect of capital and operating and maintenance costs on the component cost rate. For these components, reducing the capital and O&M cost leads to a better exergoeconomic performance. Therefore, for the PEM electrolyzer and HPG with the high f, better performance can be achieved by changing these components with another lower investing and lower exergy efficiency ones. The exergoeconomic factor of the CS reveals that by 32.43% relative cost difference is caused by the operating and maintenance cost and the remaining which is equal to 67.66% is triggered by the cost of irreversibility. For these components, it is suggested to increase the operating and maintenance cost to achieve a higher exergy efficiency and lower cost of destruction.

5. Conclusion

In the current study, a cogeneration system is investigated that consists of PVT module cells, a proton exchange membrane electrolyzer, and a double effect LiBr-H_2O absorption chiller. The cogeneration system has been analyzed from the viewpoint of the first and the second law of thermodynamics and also an extensive exergoeconomic approach. A parametric study has been performed to evaluate the effect of PV module area, solar radiation, and cell temperature on the overall exergy efficiency and total product unit cost. Furthermore, the variation of *COP* with HPG and LPG temperature, as important decision variables, is investigated on the absorption cooling and overall system performance. Finally, the exergoeconomic parameters have been calculated and the system performance has been assessed from the economic and thermodynamics points of view. The important conclusions can be summarized as:

- About 76.9% of the total exergy destruction rate refers to the PVT and the rest belongs to the double effect cooling system and PEM electrolyzer.
- Considering cooling system as a separate system, CS with 53.37% of the total exergy destruction rate has the highest destruction, which is due to the dissipative components.
- Decreasing the cell temperature improves the performance of the cogeneration system by increasing the exergy efficiency and decreasing the total product unit cost.
- In the cooling system, a better coefficient of performance can be achieved by increasing the LPG temperature and decreasing the HPG temperature.
- For the cogeneration system, the total product unit cost and overall exergy efficiency of 42.16 $/GJ and 10.56% are obtained, respectively.
- Cooling set, as a dissipative component, has the lowest exergoeconomic factor, which may be explained by the costs of exergy destruction and exergy loss.

Acknowledgement

References

[1] Pramanik S., Ravikrishna R. V., A Review of Concentrated Solar Power Hybrid Technologies, Applied Thermal Engineering (2017)127:602–637

[2] Akikur R.K., Saidur R., Ping H.W., Ullah K.R., Performance Analysis of a Co-Generation System Using Solar Energy and SOFC Technology, Energy Conversion and Management (2014)79:415–430

[3] Khanjari Y., Kasaeian A.B., Pourfayaz F., Evaluating the Environmental Parameters Affecting the Performance of Photovoltaic Thermal System Using Nanofluid, Applied Thermal Engineering (2017) 115:178–187

[4] Hazi A., Hazi G., Grigore R., Vernica S., Opportunity to Use PVT Systems for Water Heating in Industry, Applied Thermal Engineering (2014) 63: 151–157

[5] Gaur A., Tiwari G.N., Performance of a-Si Thin Film PV Modules with and without Water Flow: An Experimental Validation,
Applied Thermal Engineering (2014) 128:184–191

[6] Notton G., Cristofari C., Mattei M., Poggi P., Modelling of a Double-Glass Photovoltaic Module Using Finite Differences,
Applied Thermal Engineering (2005) 25: 2854–2877

[7] Li Z., Liu L., Liu J., Variation and Design Criterion of Heat Load Ratio of Generator for Air Cooled Lithium Bromide-Water Double Effect Absorption Chiller, Applied Thermal Engineering (2016) 96: 481–489

[8] Gomri R., Second Law Comparison of Single Effect and Double Effect Vapour Absorption Refrigeration Systems, Energy Conversion and Management (2009) 50: 1279–1287

[9] Garousi Farshi L., Mahmoudi S.M.S., Rosen M.A., Yari M., Amidpour M., Exergoeconomic Analysis of Double Effect Absorption Refrigeration Systems, Energy Conversion and Management (2013) 65:13–25

[10] Khanmohammadi S., Heidarnejad P., Javani N., Ganjehsarabi H., Exergoeconomic Analysis and Multi Objective Optimization of a Solar Based Integrated Energy System for Hydrogen Production, The International Journal of Hydrogen Energy (2017) 42: 21443–21453

[11] Penkuhn M., Spieker C., Spitta C., Tsatsaronis G., Exergoeconomic Assessment of a Small-Scale PEM Fuel Cell System, The International Journal of Hydrogen Energy (2015) 40: 13050–13060

[12] Eisavi B., Khalilarya S., Chitsaz A., Thermodynamic Analysis of a Novel Combined Cooling, Heating and Power System Driven by Solar Energy, Applied Thermal Engineering (2018)129: 1219–1229

[13] Yousefi H., Ghodusinejad M.H., Kasaeian A., Multi-Objective Optimal Component Sizing of a Hybrid ICE + PV/T Driven CCHP Microgrid, Applied Thermal Engineering (2017) 122: 126–138

[14] Akrami E., Chitsaz A., Nami H., Mahmoudi S.M.S., Energetic and Exergoeconomic Assessment of a Multi-Generation Energy System Based on Indirect Use of Geothermal Energy, Energy (2017) 124: 625–639

[15] Moradi Nafchi F., Baniasadi E., Afshari E., Javani N., Performance Assessment of a Solar Hydrogen and Electricity Production Plant Using High Temperature PEM Electrolyzer and Energy Storage, The International Journal of Hydrogen Energy (2017) 1–12

[16] Omar M.A., Altiniṣik K., Simulation of Hydrogen Production System with Hybrid Solar Collector, The International Journal of Hydrogen Energy (2016) 41: 12836–12841

[17] Nami H., Akrami E., Analysis of a Gas Turbine Based Hybrid System by Utilizing Energy, Exergy and Exergoeconomic Methodologies for Steam, Power and Hydrogen Production, Energy Conversion and Management (2017)143: 326–337

[18] Rashidi H., Khorshidi J., Xergy Analysis and Multiobjective Optimization of a Biomass Gasification-Based Multigeneration System, Energy Equipment and Systems (2018) 6: 69–87

[19] Kosmadakis G., Manolakos D., Papadakis G., Simulation and Economic Analysis of a CPV/Thermal System Coupled with an Organic Rankine Cycle for Increased Power Generation, Solar Energy (2011) 85: 308–324

[20] Ni M., Leung M.K.H., Leung D.Y.C., Energy and Exergy Analysis of Hydrogen Production by a Proton Exchange Membrane (PEM) Electrolyzer Plant, Energy Conversion and Management (2008) 49: 2748–2756

[21] Esmaili P., Dincer I., Naterer G.F., Energy and Exergy Analyses of Electrolytic Hydrogen Production with Molybdenum-Oxo Catalysts, International of Jounal of Hydrogen Energy (2012) 37: 7365–7372

[22] Saeidi S., Mahmoudi S.M.S., Nami H., Yari M., Energy and Exergy Analyses of a Novel Near Zero Emission Plant: Combination of MATIANT Cycle with Gasification Unit, Applied Thermal Engineering (2016) 108: 893–904

[23] Habibollahzade A., Houshfar E., Ashjaee M., Behzadi A., Gholamian E., Mehdizadeh H., Enhanced Power Generation through Integrated Renewable Energy Plants: Solar Chimney and Waste-to-Energy, Energy Conversion and Management (2018)166

[24] Morteza Beni H., Ahmadi Nadooshan A., Bayareh M., The Energy and Exergy Analysis of a Novel Cogeneration Organic Rankine Power and Two- Stage Compression Refrigeration Cycle, Energy Equipment and Systems (2017) 5: 299–312

[25] Behbahani-nia A., Shams S., Thermoeconomic Optimization and Exergy Analysis of Transcritical CO_2 Refrigeration Cycle with an Ejector, Energy Equipment and Systems (2016) 4: 43–52

[26] Naserian M., Farahat S., Sarhaddi F., Exergoeconomic Analysis and Genetic Algorithm Power Optimization of an Irreversible Regenerative Brayton Cycle, Energy Equipment and Systems (2016) 4: 189–203

[27] Indicators E., Marshall&Swift Equipment Cost Index, Chemical Engineering (2011) 72

[28] Akrami E., Nemati A., Nami H., Ranjbar F., Exergy and Exergoeconomic Assessment of Hydrogen and Cooling Production from Concentrated PVT Equipped with PEM Electrolyzer and LiBr-H2O Absorption Chiller, International of Journal of Hydrogen Energy (2018) 43: 622–633

[29] Misra R.D., Sahoo P.K., Gupta A., Thermoeconomic Evaluation and Optimization of a Double-Effect H2O/LiBr Vapour-Absorption Refrigeration System, In: International Journal of Refrigeration (2005) 331–343

[30] Assar M., Blumberg T., Morosuk T., Tsatsaronis G., Comparative Exergoeconomic Evaluation of Two Modern Combined-Cycle Power Plants, Energy Conversion and Management (2016) 153: 616–626

[31] Shokati N., Ranjbar F., Yari M., A Comparative Analysis of Rankine and Absorption Power Cycles from Exergoeconomic Viewpoint, Energy Conversion and Management (2014) 88: 657–668

[32] Dincer I., Rosen M.A., Ahmadi P., Optimization of Energy Systems, John Wiley & Sons (2017)

[33] Ioroi T., Yasuda K., Siroma Z., Fujiwara N., Miyazaki Y., Thin Film Electrocatalyst Layer for Unitized Regenerative Polymer Electrolyte Fuel Cells, Jounal of Power Sources (2002) 112:583–587